JOURNAL OF MATERIALS SCIENCE **34** (1999) 5613–5621

Effect of AlN and Al_2O_3 additions on the phase relationships and morphology of SiC

Part II: *Microstructural observations*

G. E. HILMAS
Department of Ceramic Engineering, University of Missouri-Rolla, Rolla, MO 65409-0330
E-mail: ghilmas@umr.edu

TSENG-YING TIEN
Department of Materials Science and Engineering, The University of Michigan, Ann Arbor, MI 48109-2136

Additions of AlN and Al_2O_3 to β-SiC hot pressed at 2100 °C strongly effect the β- to α-SiC phase transformation and the resultant α-SiC polytypes which are formed. Scanning and transmission electron microscopy were utilized to investigate the microstructural changes occurring in SiC due to these additions and to correlate these observations to their mechanical properties. The results suggest that Al_2O_3 additions stabilize the formation of the 6H-polytype of α-SiC which grows rapidly into an elongated plate-like morphology, while AlN additions stabilize the 2H-polytype of α-SiC resulting in fine equiaxed 2H-SiC : AlN solid solution grains. It is speculated that the elongated growth of 6H-SiC with Al_2O_3 additions can be controlled through the simultaneous addition of AlN. The formation of 2H-SiC : AlN solid solution grains inhibits the growth of the 6H-SiC grains since AlN(2H) will not go into solid solution in the SiC(6H) structure, effectively pinning the growth of the 6H-SiC grains.

1. Introduction

The effect of the β- to α-SiC phase transformation on the microstructural morphology of the resultant SiC grains has been shown to be strongly affected by the processing temperature and alloying or sintering additives that are utilized. The transformation from β- to α- was first observed by Baumann [1] in SiC single crystals that initially formed as β-SiC but transformed to the 6H polytype of α-SiC above 2100 °C. Many researchers have since studied the 3C to 6H transformation in producing dense polycrystalline specimens, typically with small additions of boron (B) and carbon (C), to determine the transformation mechanism and microstructural development [2–10]. Ogbuji *et al*. [9, 10] followed the nucleation of small lamellae of α-SiC and their growth into large 6H-SiC plates. As shown by Prochazka [2] and observed by all others, the final microstructure inevitably consists of a majority of highly elongated plates of 6H-SiC with finer grains of untransformed or partially transformed and heavily faulted 3C-SiC grains in between the plates. Jepps and Page [6, 7] used lattice imaging techniques to study the transformation interfaces including the intermediate structures between 3C- and 6H-SiC in single grains. Other transmission electron microscopy studies [3, 5, 10] have shown that the first stage of the transformation occurs with the formation of microtwins along the four invariant $\{111\}_\beta$ planes. When these microtwins are regularly spaced they locally become a nucleus for an α-SiC polytype leaving numerous nucleation sites for a β to α transformation, e.g. for 3C to 6H it gives rise to a $\{0001\}_{6H} \| \{111\}_{3C}$ and $[11\bar{2}0]_{6H} \| [1\bar{1}0]_{3C}$ orientation relationship with a repeat every three layers.

The 3C to 4H has been reported by numerous researchers to form in the presence of additions of aluminum (Al) [11, 12]; Al and B [13]; Al, B, and C [14, 15]; and BeO [16]. The transformation typically starts to occur above 1800 °C resulting in the expected $\{0001\}_{4H} \| \{111\}_{3C}$ and $[11\bar{2}0]_{6H} \| [1\bar{1}0]_{3C}$ orientation relationship for the formation of 4H grains. The consensus is that additions of Al or BeO increase the rate of transformation from 3C to 4H and stabilize the 4H-polytype.

The 3C to 2H transformation has raised a lot of interest in recent years largely due to the research efforts of Rafaniello *et al*. [17, 18] and Ruh and Zangvil [19]. They have shown that additions of AlN (2H), which is isostructural with the 2H polytype of SiC, causes β-SiC to preferentially transform to the 2H polytype of α-SiC. The AlN further stabilizes this polytype by forming an extensive solid solution observed to be in the range of 35 to 100 mol % AlN above 2100 °C [19]. Microstructural observations of their 2H-SiC : AlN solid solution grains has shown them to be equiaxed in morphology and typically submicron to a few microns in grain size.

The analysis of the polytypic SiC content and mechanical properties of a series of β-SiC : AlN : Al_2O_3 composites were evaluated in the first paper. This paper will focus on a microstructural investigation of this series of compositions using both scanning and transmission electron microscopy. The grain size, microstructural morphology, and intergranular content will be determined and compared with the previous X-ray diffraction phase analysis and mechanical properties results.

2. Experimental

2.1. Compositions evaluated

The nominal compositions, powder processing, and specimen fabrication techniques for the β-SiC : AlN : Al_2O_3 composites and the β-SiC : AlN and β-SiC : Al_2O_3 standards were outlined in the first paper of this series. Scanning and transmission electron microscopy were subsequently performed on the compositions that were hot pressed at 2100 °C for 1, 2, and 5 h and the standards hot pressed at 2100 °C for 1 h.

2.2. Scanning electron microscopy (SEM)

Scanning electron microscopy was performed on a Hitachi S-800* operating at 5 kV. The samples were ground and polished down to a 1 μm diamond finish and then thermally etched at 1550 °C for 20 min under 2 atm flowing nitrogen. This was found to be a reasonable etchant for revealing the SiC : SiC grain boundaries in all of the compositions. Fracture surfaces of each of the compositions were also examined by SEM from room temperature four-point bend test specimens.

2.3. Analytical electron microscopy (AEM)

AEM was performed on a JEOL 2000 FX† microscope at 200 kV equipped with a Noran‡ energy dispersive X-ray spectroscopy (EDS) system to more accurately determine the grain shape, grain morphology and chemical content of the grains for each composition. Identification of the SiC polytypes was achieved through analysis of selected area diffraction patterns (SADP's). TEM specimens were prepared from compositions in this series that were hot-pressed for 1, 2, and 5 h at 2100 °C. The specimens were ultrasonically cut into 3 mm discs from 1 mm thick sections. The discs were then mechanically ground and polished down to a thickness of 100 μm, dimpled to a 20 μm center thickness and ion milled to electron transparency using 6 kV Ar^+ ions.

3. Results and discussion

3.1. Scanning electron microscopy

Figs 1–3 are SEM micrographs outlining the changes in the microstructural morphology as the compositions changed from BS50 through BS90 after being hot pressed for 1 h at 2100 °C. Table I shows the average grain size and observed grain morphology obtained by SEM analysis along with the SiC polytypic phase content from previous XRD results. Fig. 1 shows a representative microstructure from compositions BS50, BS60 and BS70 (taken from composition BS60). These three compositions were similar in their microstructural features, containing a fine equiaxed grain morphology with little or no elongated grain formation. The average grain size was ~1.1 μm for compositions BS50 and BS60, and 1.5 μm for composition BS70. The fracture surface for all three compositions revealed very little crack deflection and a predominantly transgranular mode of fracture.

Composition BS80 exhibited a marked change in grain morphology, containing elongated 6H-SiC grains, as shown in Fig. 2. The average grain size increased to 4.0 μm with some grains achieving >7 μm in length. An increase in crack deflection was also observed providing a more intergranular mode of fracture. Fig. 3, from composition BS90, shows an even larger drastic

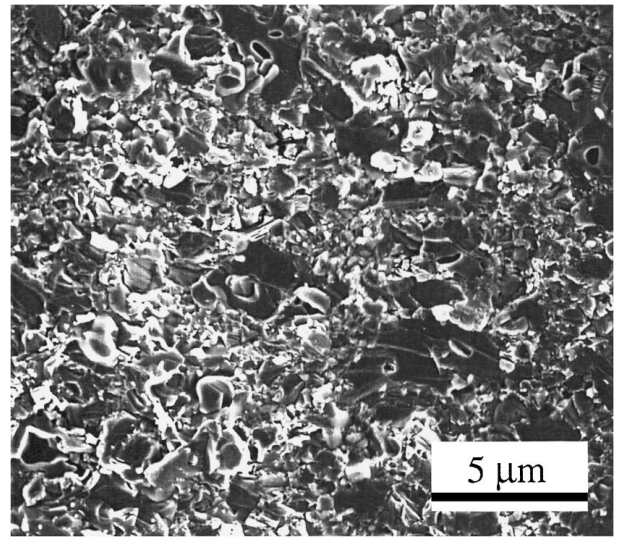

Figure 1 Representative SEM micrograph of the fracture surface of compositions BS50, BS60, and BS70 (taken from composition BS60).

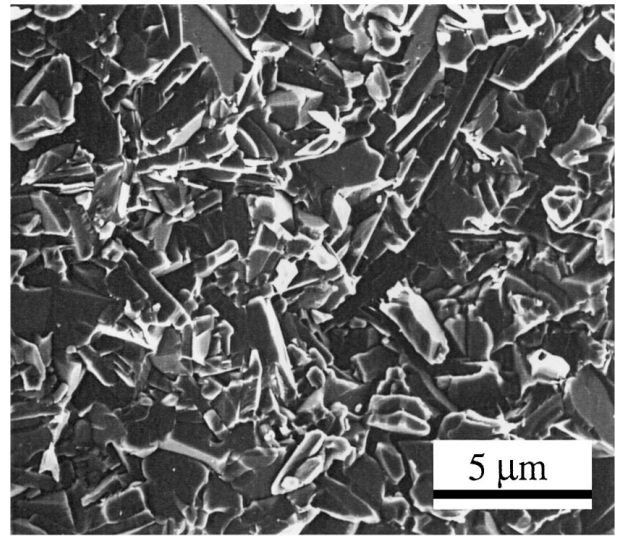

Figure 2 SEM micrograph of the fracture surface of composition BS80.

* Nissei Sangyo America, Ltd., Mountain View, CA.
† JEOL, USA, Inc., Peabody, MA.
‡ Noran, Middleton, WI.

TABLE I Grain size, grain morphology and XRD results for β-SiC : AlN : Al_2O_3 compositions

Sample code	Grain size (μm)[a]	Grain morphology	XRD results
BS50	1.1	Equiaxed	$2H_{ss}$. + minor 4H & 3C
BS60	1.1	Equiaxed	$2H_{ss}$. + minor 4H & 3C
BS70	1.5	Equiaxed	$2H_{ss}$. + minor 6H & 3C
BS80	4.0	Slightly elongated	6H-SiC + minor 2H
BS90	12.3	Elongated platelets	6H-SiC + minor 2H

[a]Using lineal analysis, but not a statistical distribution.

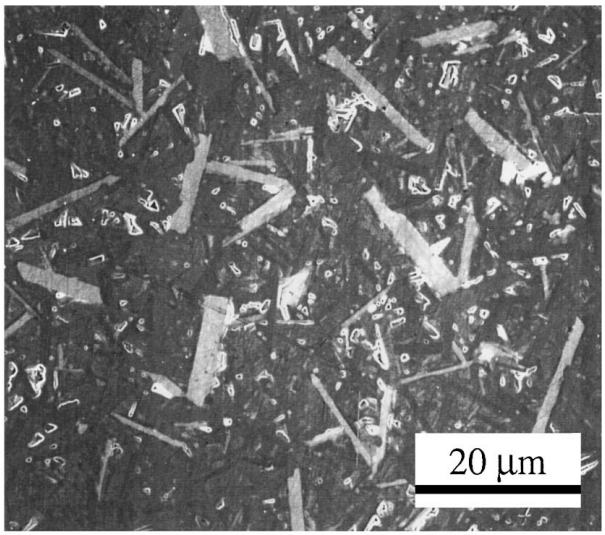

(A)

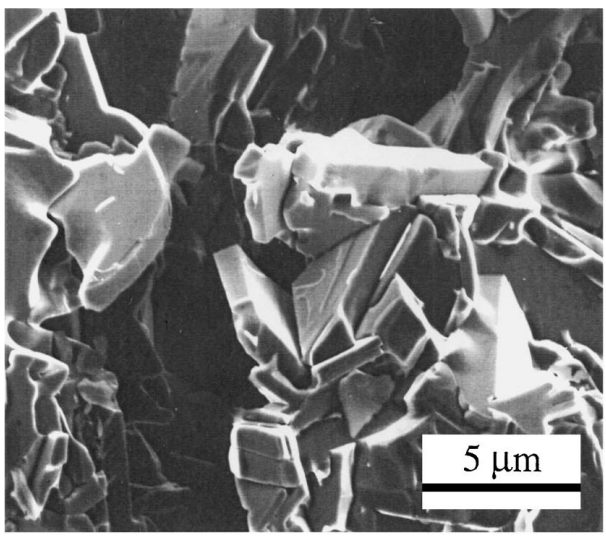

(B)

Figure 3 SEM micrographs of the polished (A) and fracture (B) surfaces of composition BS90.

increase in grain size and elongated grain morphology over composition BS80 and a pronounced intergranular fracture mode. This sample contained a majority of highly elongated 6H-SiC platelets having an average grain size of 12.3 μm. The overall microstructure contained a bimodal grain size distribution with 0.5 to 3 μm equiaxed grains that were be found between the elongated 'platelet-like' grains which were typically 10 to 20 μm in length. Despite the grain growth involved in the BS90 composition, the grains size distribution was still relatively narrow (ranging from $\sim$1 to 20 μm in length) with none of the runaway grain growth that has been observed by previous researchers during the 3C- to 6H-SiC transformation [2–5, 8, 9].

The SEM micrograph in Fig. 4, from composition BS90 : 10N, shows that 10 vol % additions of AlN to β-SiC resulted in the formation of a fine equiaxed microstructure which according XRD results were mostly 2H-SiC : AlN solid solution grains. The grain size of this composition ranged from $<$0.5 to $\sim$3.0 μm. This type of grain morphology is typical of those obtained with additions of only AlN to β-SiC [18, 20, 21].

The SEM micrograph in Fig. 5, from composition BS90:10O, shows that 10 vol % additions of Al_2O_3 to β-SiC resulted in the formation of a highly elongated microstructure. This composition contained 'platelet-like' 6H-SiC grains, many as long as 150 μm, along with somewhat finer 3 to 20 μm elongated 6H-SiC grains in between them.

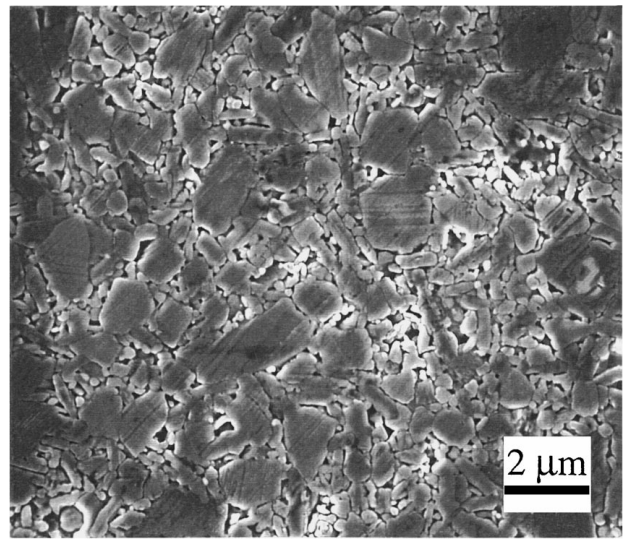

Figure 4 SEM micrograph of the microstructure of composition BS90:10N.

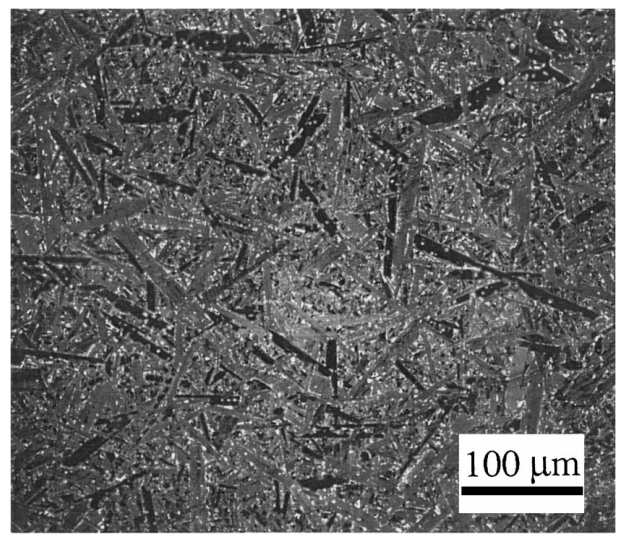

Figure 5 SEM micrograph of the microstructure of composition BS90:10O.

3.2. Transmission electron microscopy

Again, compositions BS50, BS60 and BS70 were quite similar, transforming almost exclusively to the 2H-polytype. Fig. 6, taken from BS70, is a representative bright-field image of the general microstructure of these compositions. The equiaxed 2H-polytype grains in the BS50 and BS60 compositions ranged from 0.2 to 2 μm in diameter. The BS70 composition contained a majority of equiaxed 2H-polytype grains with $\sim$20 vol % of elongated 6H-polytype grains. The 2H grains again ranged in diameter from 0.2 to 2 μm, while the 6H grains were 1 to 4 μm in length. Fig. 7 is a bright-field image of the general microstructure of the BS80 composition which transformed primarily to the 6H-polytype. Although not close to the size of the 6H-grains in the BS90 composition, these grains had also grown elongated and ranged in length from $\sim$1 to 5 μm. Fig. 8 shows a bright-field image of the general microstructure of composition BS90 which transformed almost exclusively to the 6H-polytype. These 6H SiC-polytype grew into an elongated "platelet-like" morphology with a grain size ranging from $\sim$2 to 20 μm in length. Both the BS90 and BS80 compositions also contained 2H SiC-polytype grains, $\sim$15 and 30 vol %, respectively according to XRD results. These 2H-polytype grains were equiaxed and typically $<$2 μm in size. Some β-SiC (3C) grains were also found in all five of the compositions which remained as untransformed or partially transformed from the starting

Figure 7 Bright-field TEM image of the microstructure of composition BS80.

Figure 6 Representative bright-field TEM image of the general microstructure of compositions BS50, BS60, and BS70 (taken from composition BS70).

Figure 8 Bright-field TEM image of the microstructure of composition BS90.

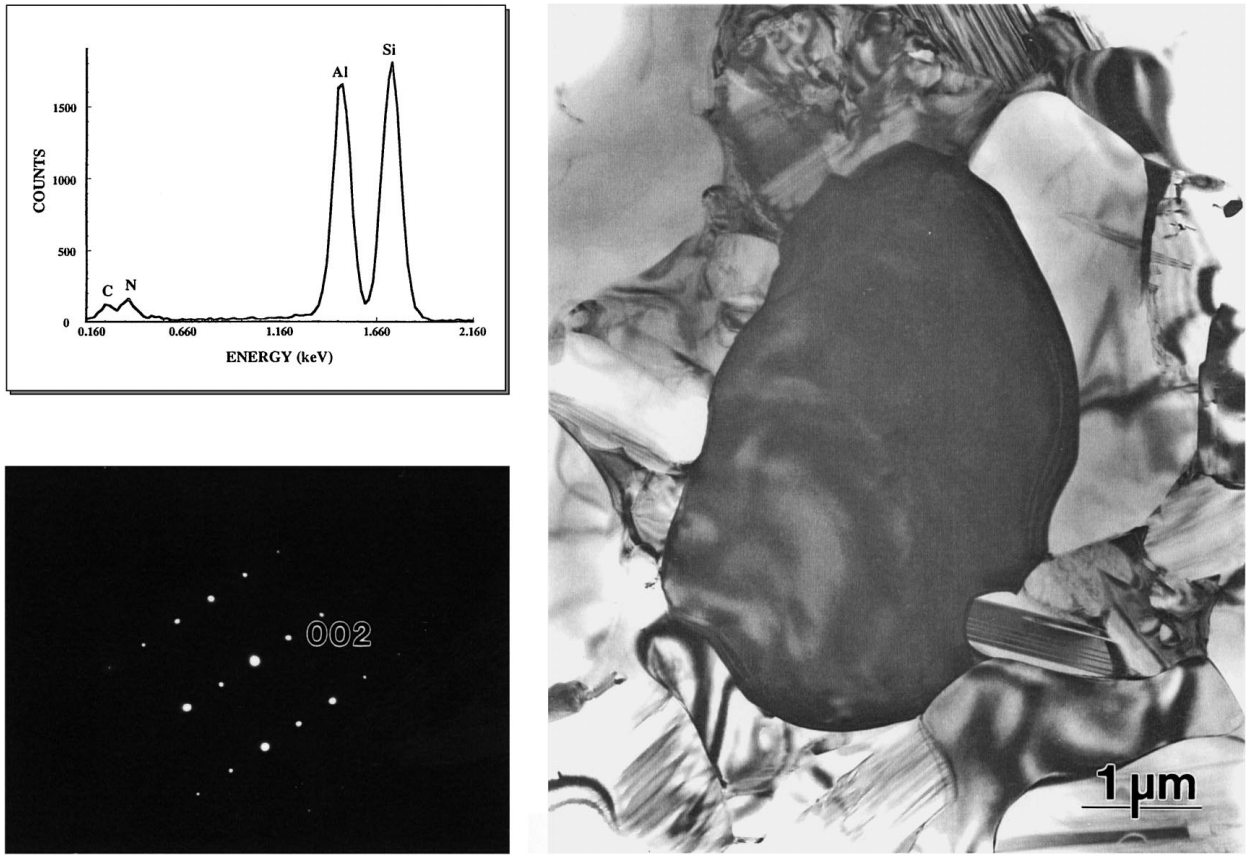

Figure 9 Bright-field TEM image, SADP, and EDS spectrum from an elongated 2H-polytype grain (Taken from composition BS60).

powder. Some of these partially transformed grains are described in more detail in the section on 'Microstructural Evolution'.

There were no pure (Si and C, only) α-SiC grains to be found in these compositions. Fig. 9 shows a bright-field image of a 2H-polytype grain from composition BS60. Included are an SADP showing the grain to be near a $[1\,\bar{2}\,13]$ zone and an EDS spectrum showing the presence of Si, Al, N, and C. This 2H grain was quite representative of the 2H-grains present in all five of the compositions, being a complete solid-solution between SiC and AlN. A bright-field image of a 6H-polytype grain from composition BS80 is shown in Fig. 10 along with a SADP near a $[1\,\bar{2}\,10]$ zone and an EDS spectrum showing that the grain contained Si, Al, O and C. This 6H-grain was representative of the 6H-grains in both the BS90 and BS80 compositions in that they all contain small amounts of Al and O. This phenomenon has been observed by previous researchers [22] in a liquid phase sintered SiC utilizing additions of Y_2O_3 and Al_2O_3. In their case, Y, Al, and O were found in the outer 'rim' of 6H-SiC grains after the specimens underwent a partial solution-reprecipitation and subsequent Ostwald ripening of the larger 6H-polytype grains during sintering at 1950 °C.

At the limits of the resolution of the equipment being used (~10 Å), a grain boundary phase was not observed at the two-grain interfaces for all of the compositions. However, there was a third crystalline phase which was located at three-grain and multi-grain junctions as shown in Fig. 11 along with its EDS spectrum (taken from composition BS80). This phase was predominant for compositions containing increasing additions of AlN and Al_2O_3. The EDS spectrum shows that the phase was high in Al and O with some Si and possibly some N present, however it remains unidentified by electron diffraction and EDS analysis.

The results of the TEM and EDS analyses agreed with the previous XRD results, and the microstructure can now be readily compared to the mechanical property results outlined in the first paper. It can be seen that there was a strong effect of an increasing grain size coupled with a decreasing strength over the series of compositions. The fine equiaxed grain morphology of the predominantly 2H-SiC : AlN solid solution grains in compositions BS50, BS60, and BS70 provided them with a high strength material achieving strengths as high as 900 MPa. Fracture toughness values for these compositions were quite low, ranging from 2.7 to 2.9 MPa-$\sqrt{\text{m}}$, and comparable to fine-grained SiC materials exhibiting little crack deflection.

BS80 was a predominantly elongated 6H-SiC matrix with ~30 vol % of fine equiaxed 2H-SiC : AlN solid solution grains. This composition provided slight improvements in the fracture toughness and the room temperature strength remained excellent at ~750 to 900 MPa. Gains in fracture toughness were likely due to the elongation of the 6H-polytype grains and an increase in the residual tensile stress at the grain boundary providing increased crack deflection behavior as shown in Fig. 2.

Composition BS90 contained mostly elongated 6H-SiC grains but exhibited no runaway grain growth due to the close proximity of the 2H-SiC : AlN solid solution

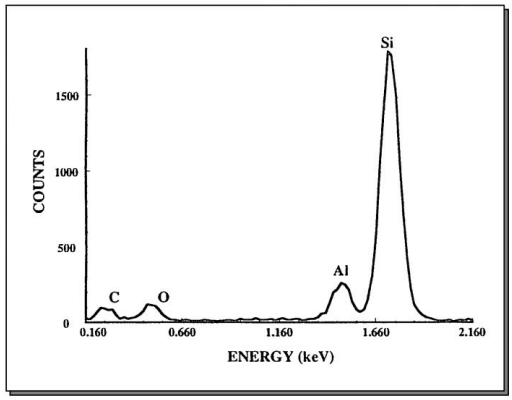

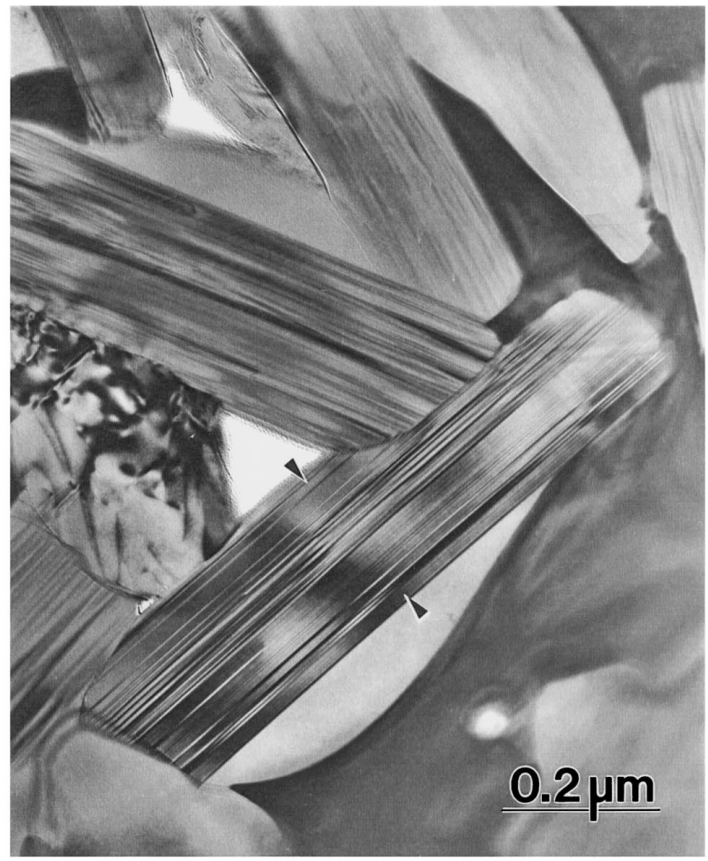

Figure 10 Bright-field TEM image, SADP, and EDS spectrum from an elongated 6H-polytype grain (Taken from composition BS80).

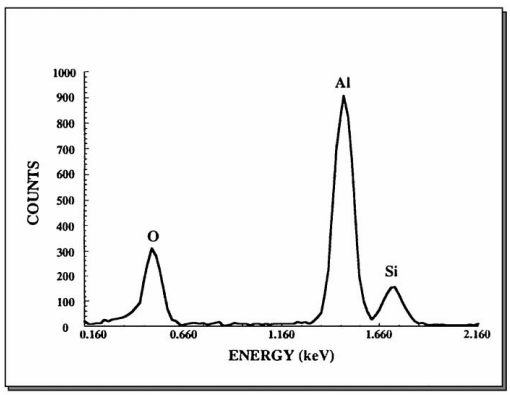

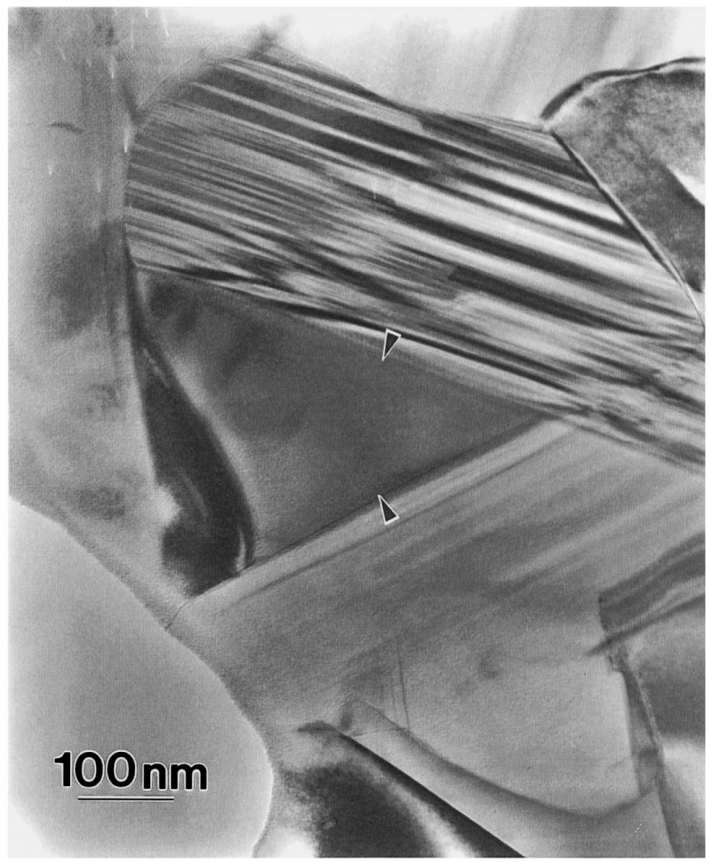

Figure 11 Bright-field TEM image and EDS spectrum from the grain boundary phase located at three-grain and multi-grain junctions in all five of the compositions (Taken from composition BS80).

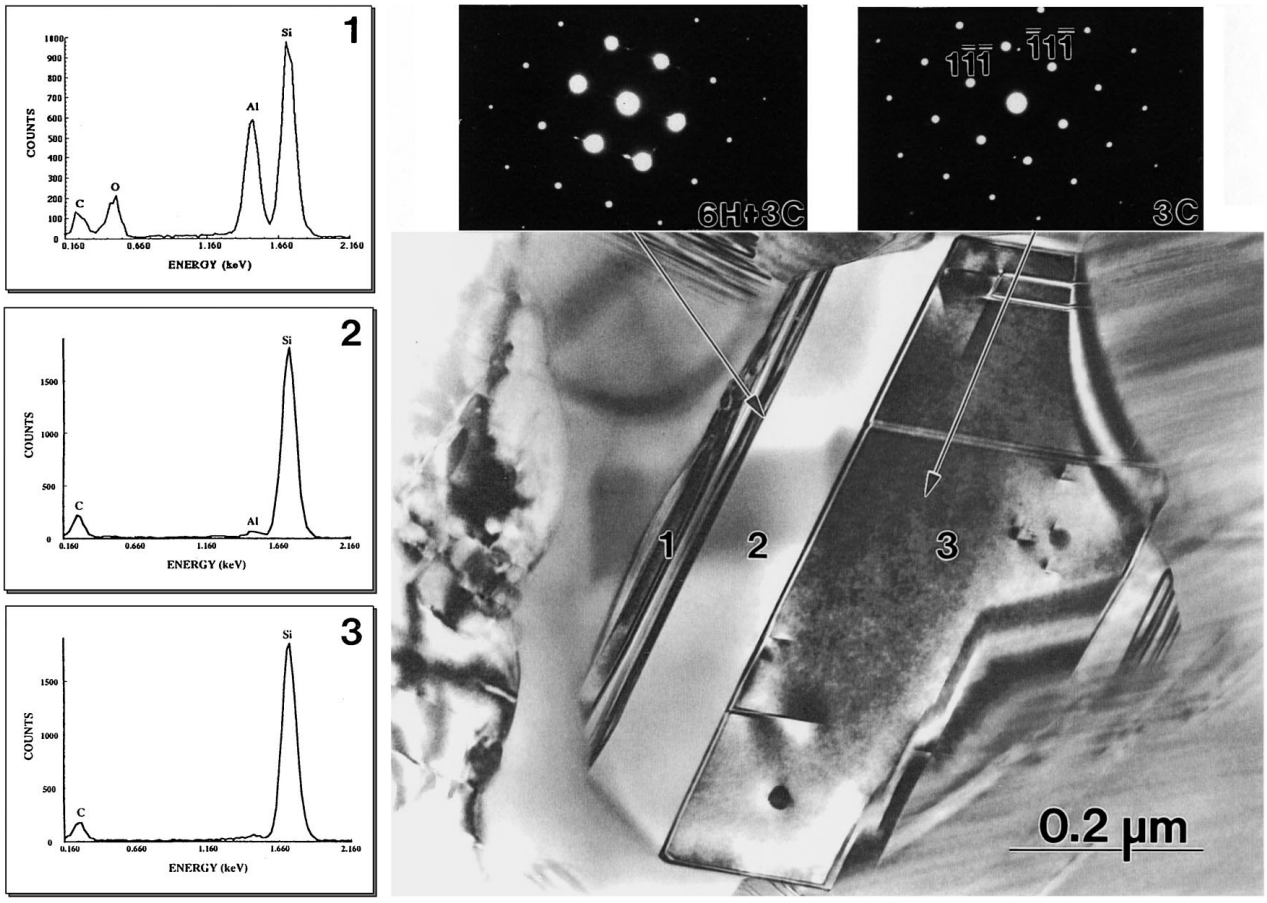

Figure 12 Bright-field TEM image and EDS spectra of a partially transformed β-SiC (3C) grain from composition BS80 showing how the elongated 6H-SiC grains are forming from the original 3C-SiC grains.

grains. The 6H grains provided the elongated grains required to deflect the advancing crack while the 2H grains controlled the overall length of the 6H grains by acting as grain growth inhibitors. The 6H grains were unable to grow through the 2H grains since these contained AlN in solid solution and the 2H-AlN would not go into solid solution with the 6H-polytype of SiC. The high fracture toughnesses ($\sim$9 MPa-$\sqrt{\text{m}}$) have already been shown to be attributed to strong increases in crack deflection around the 6H-SiC grains. Also, the uniformity of the microstructure still provided room temperature flexural strengths as high as 600 MPa, more than twice what would be predicted by an inverse square root relation between strength and grain size as compared to the other compositions.

The flexural strength versus grain size for the BS50 through BS90 compositions definitely does not follow an inverse square root relationship with grain size. As pointed out in the first paper, this result tends to show that microcracks may play an important role in these materials and may very well control their overall strengths, at least for the large grain compositions.

3.3. Microstructural evolution

All of the compositions contained a few untransformed or partially transformed grains of β-SiC (3C). Microstructural observations of these transforming grains has led to a broader understanding of the morphology of the developing microstructure, particularly for the formation of elongated α-SiC plates [4, 5, 8–10]. Fig. 12 is a TEM micrograph of a partially transformed β-SiC grain from composition BS80 that shows how the elongated 6H-SiC grains were forming from the original 3C-SiC grains. Region 3 shows a large area of untransformed β-SiC as shown by the [110] SADP (arrowed) and the Si and C peaks in the EDS spectrum. Twin boundaries have formed in several areas of region 3 along the $\{111\}_\beta$ twinning planes of the 3C structure. The 70° angle is indicative of this type of twinning since it is the angle between the four invariant $\{111\}_\beta$ planes in the 3C structure. Region 2 has basically become a twin to region 3 down the long axis of the crystal. The EDS spectrum from region 2 shows that it still contained only Si and C. Stronger faulting and twin formation has occurred in region 1, to the left of region 2, giving rise to transformation to and growth of the 6H polytype of α-SiC. The inset SADP (arrowed between regions 1 and 2) shows the 3C-SiC from region 2 and streaking perpendicular to $(1\,\underline{1}\,\underline{1})_\beta$ due to the parallel growth of $(0006)_{6H}$ from region 1. It can be seen from the EDS spectrum of region 1 that the 6H polytype grew with concurrent additions of Al and O into its structure from the surrounding Al, Si, O containing grain boundary phase.

Fig. 13 shows another of these partially transformed 3C-SiC grains from composition BS70. The regions of 3C- and 6H-SiC have been labeled, and it can be seen that parallel growth of more than one grain of 6H-SiC has occurred and these grains were starting to grow and

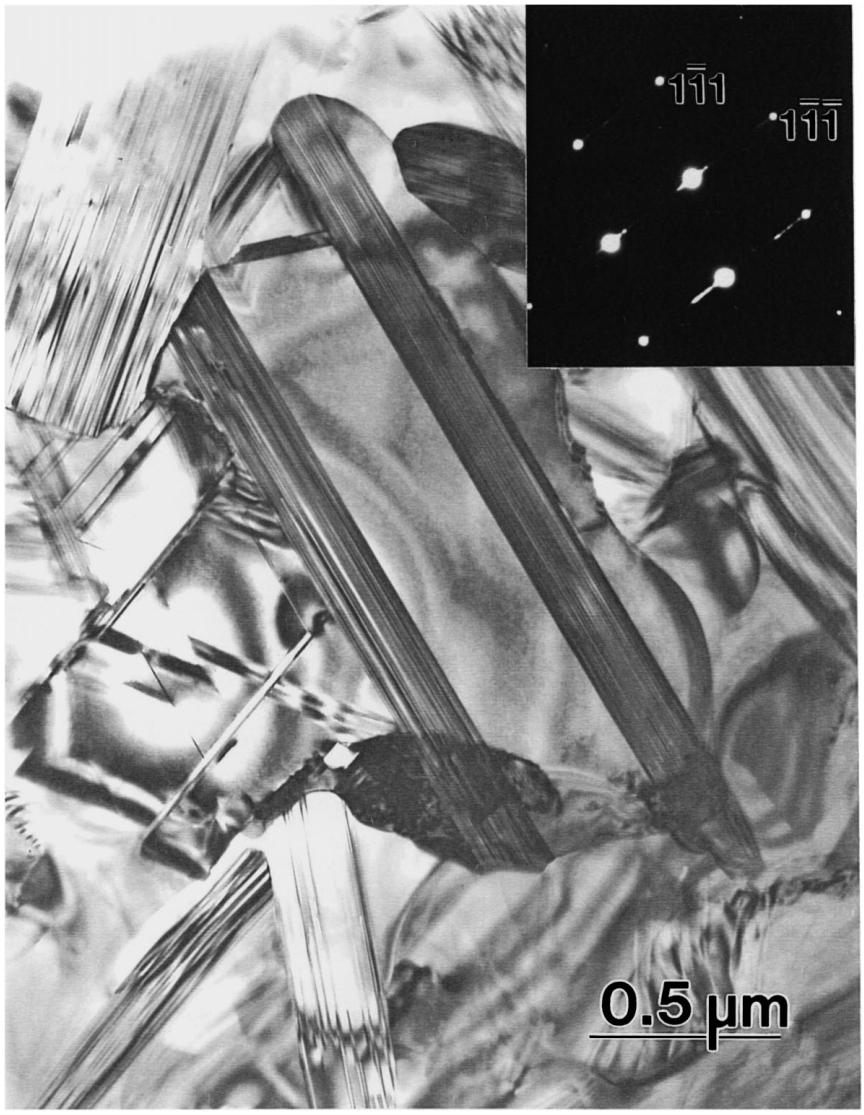

Figure 13 Bright-field TEM image of a partially transformed β-SiC (3C) grain from composition BS70 showing how the elongated 6H-SiC grains are forming from the original 3C-SiC grains.

extend beyond the 3C-SiC grain from which they were formed. The inset SADP is a [110] zone from the 3C-SiC grain along with streaking perpendicular to $(1\,\bar{1}\,1)_\beta$ from the (0006) planes of the 6H-SiC.

4. Conclusions

On the basis of the present work, the following conclusions can be drawn:

(1) SEM and TEM results have shown that large additions of AlN and Al_2O_3 (i.e. >30 vol % 3AlN : Al_2O_3) to β-SiC hot pressed at 2100 °C results in the formation of a majority of 2H-SiC grains which contain Al and N in solid solution. Compositions in this range have an average grain size of $\leq$1.5 μm. Fracture surfaces reveal predominantly transgranular fracture, indicative of their low fracture toughness values of <3 MPa-$\sqrt{\text{m}}$.

(2) Compositions containing 20 vol % of 3AlN : Al_2O_3 additives exhibited increases in grain size to >4 μm due to the formation of elongated 6H-SiC grains. Fracture surfaces revealed an increase in intergranular fracture which resulted in fracture toughnesses of >5 MPa $\sqrt{\text{m}}$.

(3) Compositions containing 10 vol % of 3AlN:Al_2O_3 additives showed a marked increase in average grain size to >12 μm. A two phase microstructure exists consisting of >85 vol % of 6H-SiC grains with the remainder being mostly 2H-SiC grains. The 6H-SiC grains have an elongated platelet morphology and are typically 10 to 20 μm in length and contain small quantities of Al and O in their structure. The 2H-SiC grains are equiaxed in morphology, typically <2 μm in size, and contain large quantities of Al and N in solid solution. Fracture surfaces showed strong effects of crack deflection around the elongated 6H grains providing fracture toughness increases to 9 MPa μm.

(4) Additions of only 10 vol % AlN to SiC resulted in fine equiaxed 2H-SiC : AlN solid solution grains. Additions of only 10 vol % Al_2O_3 to SiC provided transformation to predominantly 6H-SiC which grew into a highly elongated platelet morphology with grains achieving >150 μm in length.

(5) The elongation of 6H-SiC with Al_2O_3 additions can be controlled through the addition of AlN. AlN caused β-SiC (3C) to preferentially transform to the 2H polytype of SiC providing smaller equiaxed 2H-SiC : AlN solid solution grains which inhibit the growth

of the 6H grains since AlN (2H) will not go into solid solution in SiC (6H). This premise provides the ability to control the phase content, microstructural morphology, and thus the mechanical properties of SiC-based composites through simultaneous additions of AlN and Al_2O_3.

Acknowledgement

Supported by U.S. Department of Energy, Office of Transportation Technologies, Advanced Materials Development Program under Contract No. DE-AC05-84OR2140, administered by D. R. Johnson of Oak Ridge National Laboratory.

References

1. H. N. BAUMANN, Jr., *J. Electrochem. Soc*. **99** (1952) 109–114.
2. S. PROCHAZKA, in Proc. of the Int'l Conf. on Silicon Carbide (University of South Carolina Press, Columbia, SC, 1973) pp. 394–402.
3. C. A. JOHNSON and S. PROCHAZKA, in Proc. of the 6th Int'l Materials Symp., "Ceramic Microstructures '76", edited by R. M. Fulrath and J. A. Pask (Westview Press, Boulder, CO, 1977) pp. 366–378.
4. K. R. KINSMAN and S. SHINOZAKI, in Proc. of the Int'l Conf. on Solid State Phase Transformations, edited by H. Aaronson (Carnegie-Mellon University, Pittsburgh, PA, 1983) pp. 605–609.
5. *Idem*., in Proc. of the 14th Univ. Conf. on Ceramic Science of Processing of Crystalline Ceramics, edited by H. Palmer, R. F. Davis, and T. M. Hare (North Carolina State University, Raleigh, NC, 1977) pp. 641–652.
6. N. W. JEPPS and T. F. PAGE, *J. Microsc*. **116** (1979) 159–171.
7. *Idem*., *ibid*. **119** (1980) 177–188.
8. A. H. HEUER, G. A. FRYBURG, L. U. OGBUJI, T. E. MITCHELL and S. SHINOZAKI, *J. Amer. Ceram. Soc*. **61** (1978) 406–412.
9. L. U. OGBUJI, T. E. MITCHELL and A. H. HEUER, *ibid*. **64** (1981) 91–99.
10. L. U. OGBUJI, T. E. MITCHELL, A. H. HEUER and S. SHINOZAKI, *ibid*. **64** (1981) 100–105.
11. K. A. SCHWETZ and A. LIPP, in Proceedings of the 10th Symposium on the Science of Ceramics, edited by H. Hausner (Deutsche Keram. Ges., Germany, 1980) pp. 149–158.
12. M. MITOMO, Y. INOMATA and H. TANAKA, *Mat. Res. Bull*. **6** (1971) 759–764.
13. D. H. STUTZ, S. PROCHAZKA and J. LORENZ, *J. Amer. Ceram. Soc*. **68** (1985) 479–482.
14. S. SHINOZAKI, R. M. WILLIAMS, B. N. JUTERBOCK, W. T. DONLON, J. HANGAS and C. R. PETERS, *Amer. Ceram. Soc. Bull*. **64** (1985) 1389–1393.
15. S. SHINOZAKI, J. HANGAS, J. MAEDA and A. SOETA, in "Ceramic Transactions," Vol. 2, *Silicon Carbide '87*, edited by J. W. Cawley and C. E. Semler (The American Ceramic Society, Westerville, OH, 1989) pp. 113–121.
16. Y. TAKEDA, K. USAMI, K. NAKAMURA, S. OGIHARA, K. MAEDA, T. MIYOSHI, S. SHINOZAKI and M. URA, in "Advances in Ceramics," Vol. 7, edited by M. F. Yan and A. H. Heuer (The American Ceramic Society, Westerville, OH, 1983) pp. 253–262.
17. W. RAFANIELLO, M. R. PLICHTA and A. V. VIRKAR, *J. Amer. Ceram. Soc*. **66** (1983) 272–276.
18. W. RAFANIELLO, K. CHO and A. V. VIRKAR, *J. Mater. Sci*. **16** (1981) 3479–3488.
19. R. RUH and A. ZANGVIL, *J. Amer. Ceram. Soc*. **65** (1982) 260–265.
20. W. RAFANIELLO, A PhD dissertation, The University of Utah, June, 1984.
21. Y. XU, A. ZANGVIL, M. LANDON and F. THEVENOT, *J. Amer. Ceram. Soc*. **75** (1992) 325–333.
22. L. S. SIGL and H.-J. KLEEBE, *ibid*. **76** (1993) 773–776.

Received 1 October 1997
and accepted 18 August 1998